DOI: 10.1002/chem.200802107

Electron Donation in the Water–Water Hydrogen Bond

Rustam Z. Khaliullin,*[a] Alexis T. Bell,[b] and Martin Head-Gordon*[c]

Hydrogen bonding is central to aqueous systems, from small water clusters and microsolvated ions to bulk water, and solvated biomolecules.[1] Despite numerous experimental and theoretical studies, the physical nature of hydrogen bonding is still debated. One issue is the extent of intermolecular charge transfer (CT) in hydrogen bonding.[2] Natural bond orbital (NBO) analysis[3] and natural energy decomposition analysis[4] suggest that CT is predominant[5,6] because, if CT is neglected, NBO analysis shows no binding at the water-dimer equilibrium geometry. However, other earlier decomposition methods[7,8] estimated that CT contributes only around 20% of the overall binding energy.[8,9] This question has practical significance for aqueous molecular dynamics simulations, where models based on purely electrostatic potentials, such as Coulomb plus Lennard-Jones with perhaps polarizability, seem to be very successful in reproducing many structural and thermodynamic properties of water.[10] Is such good agreement soundly based or fortuitous?

Recent X-ray absorption and X-ray Raman scattering experiments have challenged the accepted locally tetrahedral structure of liquid water.[11] The failure of classical molecular dynamics simulations to reproduce the "chain and ring" local structure inferred from these experiments has generated questions about the reliability of existing water potentials.[5,11,12] This fact, combined with the CT character of the hydrogen bonding suggested by NBO analysis, has led to proposals to incorporate CT effects into empirical water potentials.[5] However, the "chain and ring" interpretation of the X-ray experiments is highly controversial and has been challenged on many fronts.[13]

Herein, we rationalize the success of empirical electrostatic potentials by clarifying intermolecular CT effects in the simplest water cluster, the water dimer. We have used our recently developed energy-decomposition analysis (EDA)[14] and charge-transfer analysis (CTA)[15] based on absolutely localized molecular orbitals (ALMOs),[16,17] which are ideal for separating CT from frozen density and polarization interactions. In ALMO EDA, the frozen density (FRZ) term is calculated as the interaction energy of the unrelaxed electron densities on the molecules. The polarization (POL) term is due to the deformation (or polarization) of the electron clouds of the molecules in the field of each other. Quantum mechanically, it is described as the energy lowering due to the *intramolecular* relaxation of each molecule's ALMOs in the field of the other molecule. CT is calculated as the energy lowering due to the *intermolecular* relaxation of the molecular orbitals corrected for the basis set superposition error (BSSE).[14,15]

Like related earlier methods,[7,8] the ALMO atomic-to-molecular orbital transformation is constrained to be block-diagonal in terms of the molecular fragments (prohibiting CT). Unlike those earlier methods, ALMO EDA and CTA treat the optimization of the ALMO's in a variationally optimal way.[14,15,18] CT effects (energy lowering due to electron transfer from occupied orbitals on one molecule to virtual orbitals of another molecule, and then any further repolarization or higher-order relaxation) are corrections to the optimal polarized reference system, and cannot be over or underestimated. The ALMO charge transfer scale, ΔQ, provides a measure of the distortion of the electronic clouds upon formation of an intermolecular bond and is such that all CT terms, that is, forward-donation, back-donation, and higher order relaxation, have well defined energetic effects.[15]

The water dimer geometry with C_s symmetry was optimized at the MP2/aug-cc-pVQZ level. All calculations were

[a] Dr. R. Z. Khaliullin
Department of Chemistry, University of California Berkeley
Berkeley, CA 94720 (USA)
Fax: (+1) 510-643-1255
E-mail: rustam@khaliullin.com

[b] Prof. A. T. Bell
Department of Chemical Engineering, University of California Berkeley
Berkeley, CA 94720 (USA)

[c] Prof. M. Head-Gordon
Department of Chemistry, University of California Berkeley
Berkeley, CA 94720 (USA)
Fax: (+1) 510-643-1255
E-mail: mhg@bastille.cchem.berkeley.edu

Supporting information for this article is available on the WWW under http://dx.doi.org/10.1002/chem.200802107.

performed with the Q-Chem software package.[19] The relative position of the molecules in the dimer is described by three parameters (Figure 1 A). The MP2/aug-cc-pVQZ

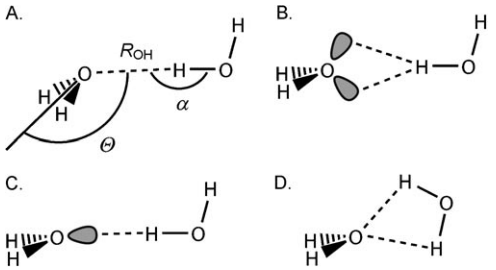

Figure 1. Water molecules in the water dimer.

structure is characterized by $\alpha = 172°$, $\Theta = 127°$, and $R_{OH} = 1.94$ Å. Since ALMO methods are presently limited to single determinant wavefunctions, we applied decomposition analysis to wavefunctions calculated with a series of density functionals (see the Supporting Information). Although the CT contribution somewhat depends on the chosen density functional (just as the binding energies do), the main qualitative conclusions of this study remain the same for all commonly used density functionals. Therefore, we further discuss results obtained with the B3LYP density functional (Table 1). This functional most closely reproduces more accurate MP2 water-dimer binding energies of the various functionals that we tried.

Table 1. ALMO CTA and EDA results for the water dimer. Geometry is optimized at the MP2/aug-cc-pVQZ level, decomposition analysis is performed at the B3LYP/aug-cc-pVXZ level (X = D, T, Q, 5). All terms are corrected for BSSE.

Scale	ΔQ [mē]				ΔE [kJ mol^{-1}]			
X	D	T	Q	5	D	T	Q	5
FRZ		0.0			-5.5	-5.4	-5.2	-5.1
POL		0.0			-4.5	-6.1	-6.5	-7.1
CT(A→D)[a]	0.1	0.2	0.1	0.1	-0.2	-0.4	-0.3	-0.2
CT(D→A)[a]	3.7	2.4	2.8	2.7	-7.9	-6.6	-6.6	-6.3
Rem. CT[b]	0.3	0.2	-0.4	-0.5	-0.4	-0.3	-0.3	-0.3
Total[c]	**4.0**	**2.7**	**2.5**	**2.3**	**-18.5**	**-18.8**	**-18.9**	**-18.9**
BSSE	0.3	0.1	0.0	0.0	1.0	0.2	0.1	0.0
COVP$_1$[d]	95	97	96	97	90	97	93	96

[a] D = electron donor, A = electron acceptor; [b] Remaining CT includes intramolecular terms as well as the higher order relaxation term; [c] MP2 interaction energies are −18.3, −19.8, and −20.6 kJ mol^{-1} for X = D, T, and Q, respectively; [d] Contribution of COVP$_1$ is given as percentage of CT(D→A).

The results of the B3LYP ALMO decomposition analysis show that the energy and charge components rapidly converge as the basis set becomes locally complete, indicating stability of the ALMO decomposition (Table 1). All CT terms presented in the paper are corrected for BSSE. The BSSE is presented in Table 1 to show the degree of basis set completeness. The very small values of BSSE suggest that the aug-cc-pVQZ and aug-cc-pV5Z basis sets are effectively complete for our present purpose.

It is clear that all energy components (frozen density, polarization, and charge-transfer) are important for energetic stabilization of the dimer at its equilibrium geometry (Table 1). We therefore conclude that the NBO approach significantly overestimates CT due to nonvariational treatment of the reference "zero CT" electronic state. Our results show that CT contributes around 36% of the overall binding energy in the complete basis set limit, of which approximately 95% is from the proton acceptor to the proton donor. The same effect occurs on the charge scale, indicating a direct correspondence between electron redistribution and the energy of CT interactions, which is not always the case.[15]

The total electron density transfer calculated with ALMO CTA is just a few millielectrons (2.3 mē at the B3LYP/aug-cc-pV5Z level). This result is an order of magnitude smaller than the CT calculated with the Mulliken, Löwdin, and natural population analysis (PA) methods (Table 2).[20] This discrepancy arises largely from the different meaning assigned to CT in ALMO CTA and PA methods. ALMO CTA measures CT as the degree of electron relaxation from the optimal polarized (pre-CT) state to the delocalized state. In contrast, PA methods include not only true CT, but also the separate (and in this case larger) effect of partitioning the charge distribution of the polarized pre-CT state (for a detailed comparison see Ref. [15]). Thus the key advantage of the ALMO CTA approach is that it shows the electron transfer associated with energy lowering due to dative interactions: just a few millielectrons.

Table 2. Charge (mē) of the electron-acceptor molecule in the dimer. Geometry is optimized at the MP2/aug-cc-pVQZ level, population analysis is performed at the B3LYP/aug-cc-pVXZ level (X = D, T, Q, 5). All charges are corrected for BSSE.

X	D	T	Q	5
Mulliken PA	-27.5	-18.8	-22.2	-17.0
Löwdin PA	-24.0	-24.0	-21.2	-17.8
Natural PA	-18.3	-16.5	-17.1	–

Whereas it may seem remarkable that so little CT (2.7 mē D→A) can stabilize the hydrogen bond by 6.3 kJ mol^{-1} (equivalent to 24 eV per electron) it is quite consistent with simple estimates from perturbation theory. The CT energy is a second order correction to the energy of the polarized system, and is proportional to $F_{ad}^2/(\varepsilon_a - \varepsilon_d)$,[14] where F_{ad} is the CT energy coupling between donating orbital d and accepting orbital a, and ε_i is the energy of orbital i. The ΔQ term is proportional to the square of the single excitation amplitude, $F_{ad}^2/(\varepsilon_a - \varepsilon_d)^2$.[15] Therefore, the CT energy per electron is related to the energy gap between donating and accepting orbitals $\varepsilon_a - \varepsilon_d$. The B3LYP/aug-cc-pV5Z energy gap between the most important donating and accepting orbitals in the water dimer lies between 10 and 40 eV (virtual orbitals in such a big basis set practically form a contin-

uum of states). Thus, a value of 24 eV for the effective *d–a* gap for CT between water molecules in the dimer at the equilibrium geometry is entirely reasonable.[21]

Complementary occupied–virtual orbital pairs (COVPs)[15] allow us to visualize CT effects and provide additional insight into the nature of hydrogen bonding in the water dimer. Each COVP corresponds to an occupied orbital on one molecule donating charge to one specific (complementary) virtual orbital on the other molecule. COVPs provide the best compact orbital description of CT between a pair of molecules. In the water dimer, only one COVP is significant, and accounts for 96–97% of the overall transfer from proton acceptor to proton donor on the energy and charge scales (Table 1). The remaining CT in this direction is attributable to the four remaining complementary occupied–virtual pairs, none of which exceeds 3% of the overall transfer.

The shapes of the occupied and the virtual orbitals of the main COVP are shown in Figure 2 ($\Theta = 127°$). The virtual

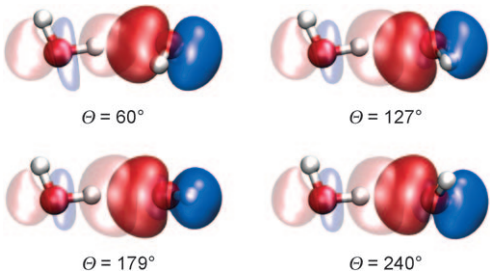

Figure 2. Dependence of the shape of the most significant COVP on the relative orientation of the water molecules in the dimer. All figures show orbitals calculated at the B3LYP/aug-cc-pVQZ level, with an isosurface value of 0.05. Occupied orbitals are represented by intense colors. Faint areas represent complementary virtual orbitals.

orbital strongly resembles the O–H antibonding orbital, σ^*_{OH}, of the electron-accepting molecule. This is consistent with oxygen atom lone pairs donating electron density to the antibonding orbitals of the other molecule. However, the donating orbital is interesting and unexpected because it does not resemble an sp^3-hybridized lone pair. In predicting molecular geometries (VSEPR), sp^3-hybrids play an important role and sp^3-hybridized lone pairs on the O atom arise from ab initio calculations when finding the most localized occupied orbitals of water molecules.[22]

However, the occupied orbitals are not unique, and can therefore be fixed by criteria that include ionization energy (giving canonical orbitals, Figure 3), maximal localization (giving sp^3 lone pairs), or the most compact representation of CT effects (the COVP shown in Figure 2). The COVP is best suited for studying donor–acceptor interactions, and the form of the optimal donor and acceptor orbitals can be understood as a compromise between high energy and good interaction with the acceptor. In this regard, we can see that the optimal acceptor orbital (Figure 2) bears almost no resemblance to the low-lying canonical virtual orbitals

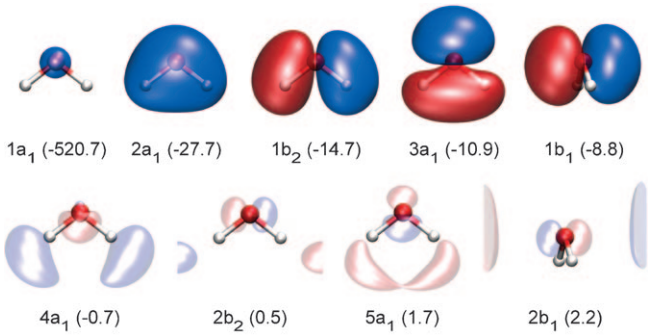

Figure 3. Symmetry of the five occupied and the lowest four virtual canonical molecular orbitals of molecule. Orbital energies (eV) are shown in parentheses. See Figure 2 for full description.

(Figure 3), consistent with the effective *d–a* gap being far larger than the HOMO–LUMO gap. The occupied (donating) orbital is mostly a linear combination of $3a_1$ and $1b_1$ canonical orbitals (Figure 3) that are the two highest lying orbitals of the electron-donating water molecule. A small CT contribution from the $2a_1$ canonical orbital of the donating molecule, which is a combination of the oxygen 2s orbital and hydrogen 1s orbitals, is reasonable given that its low energy makes it a poor donor. This simple argument explains the form of the donating orbital in the water dimer complex (Figure 2, $\Theta = 127°$).

Further support for this interpretation comes from the dependence of the B3LYP/aug-cc-pVQZ BSSE corrected energy and its ALMO decomposition on the orientation of the water molecules (Figure 4, Θ is varied and all other internal coordinates remain fixed at their MP2/aug-cc-pVQZ values). The CT energy does not maximize around tetrahedral coordination ($\Theta = 127°$). The energy lowering due to the most significant COVP changes remarkably little from

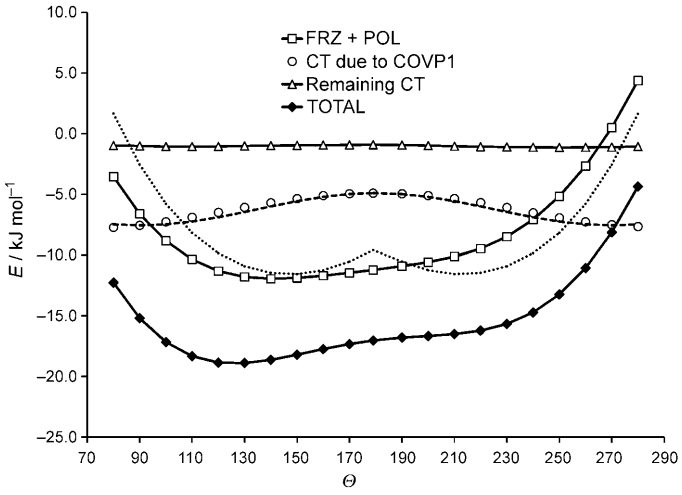

Figure 4. Dependence of the energy components on the relative orientation of water molecules in the dimer. B3LYP/aug-cc-pVQZ. – – – CT calculated according to Equation (1). ····· FRZ+POL interactions calculated according to Equation (2).

$-4.9\ \mathrm{kJ\,mol^{-1}}$ for $\Theta = 180°$ to $-7.7\ \mathrm{kJ\,mol^{-1}}$ for $\Theta = 50°$. From Figure 2, the donor orbital does not rotate with the water molecule but stays directed towards the electron accepting molecule, unlike an sp^3 lone pair. The principal donor orbital thus changes with rotation to optimize the coupling with the complementary σ^*_{OH} virtual acceptor orbital, thereby explaining the weak dependence of the CT energy on Θ.

It is interesting to consider hydrogen bonds that involve bifurcated interactions. $\Theta = 179°$ corresponds to an OH bond interacting with two sp^3 lone pairs, a bifurcated donor, in the traditional manner (Figure 1B). However, the CT contribution to H-bonding still involves only one donating orbital (Figure 2, Figure 1C). The reduction in CT energy at $\Theta = 179°$ reflects a greater contribution from the lower energy $3a_1$ orbital and a decreased contribution from the highest occupied $1b_1$ orbital of the donor molecule. In fact, the dependence on Θ of CT energy can be well represented as a linear combination of CT from these two orbitals (Figure 4, – – –) given by Equation (1):

$$\Delta E_{D\rightarrow A}(\Theta) = \Delta E_{1b_1}\sin^2(\Theta) + \Delta E_{3a_1}\cos^2(\Theta) \quad (1)$$

The shape of the FRZ curve can be explained in purely electrostatic terms. The dotted line in Figure 4 represents the interaction energy of point charges placed at the position of the nuclei in the dimer (-1.0 ē and $+0.5$ ē charges replace O and H atoms correspondingly, Figure 4, •••••) is given by Equation (2):

$$\Delta E_{(FRZ+POL)}(\Theta) = \Sigma_{i\in D}\Sigma_{j\in A}\frac{q_i q_j}{r_{ij}} + 29.2\ \mathrm{kJ\,mol^{-1}} \quad (2)$$

The constant in the equation is included to capture effects that are essentially independent of Θ, such as polarization and exchange (ΔE_{POL} dependence on Θ is shown in Ref. [14]). Therefore, we conclude that the position of the minimum on the total energy curve at $\Theta = 127°$ is determined by a combination of both electrostatic and charge-transfer interactions.

In the case of a bifurcated acceptor (Figure 1D), the description changes qualitatively. The CT term becomes very small due to poor interactions and has significant contributions from two COVPs (Figure 5); the symmetric ($3a_1$ canonical orbital, Figure 3) and antisymmetric ($1b_1$ canonical orbital, Figure 3). This reflects the availability of two acceptor antibonding σ^*_{OH} (symmetric $4a_1$ and antisymmetric $2b_2$) orbitals in the vicinity of the electron-donating molecule. In larger water clusters, bulk liquid water, and ice, the donating orbitals will change their shape and orientation according to the local environment.

In summary, we have applied a new variation-based energy decomposition and charge-transfer analysis to study intermolecular CT effects in the hydrogen bond between two water molecules, using density functional calculations. Our main conclusions are as follows:

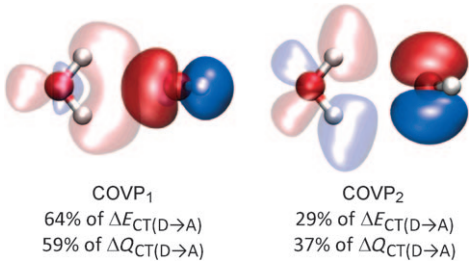

Figure 5. Bifurcated hydrogen bonding in the water dimer. EDA terms ($\mathrm{kJ\,mol^{-1}}$): $\Delta E_{FRZ} = -8.2$, $\Delta E_{POL} = -1.7$, $\Delta E_{CT(D\rightarrow A)} = -0.9$, $\Delta E_{CT(A\rightarrow D)} = -0.2$, $\Delta E_{TOTAL} = -11.0$. CTA terms (mē): $\Delta Q_{CT(D\rightarrow A)} = 0.4$, $\Delta Q_{CT(A\rightarrow D)} = 0.1$, $\Delta Q_{TOTAL} = 0.5$. See Figure 2 for full description.

1) Although CT effects play an important role in hydrogen bonding they are not solely responsible for the energetic stabilization of $(H_2O)_2$. The contributions of frozen density interactions and polarization are not less significant than that of CT, unlike some earlier work.[5,6]

2) The amount of intermolecular CT is on the order of a few millielectrons, which is much smaller than has been inferred from population analysis. Furthermore, the CT is fairly insensitive to intermolecular rotation of the water molecules, which helps to account for the success of empirical potentials that do not include charge transfer explicitly.

3) Complementary occupied–virtual pairs (COVPs) provide a new and satisfying view of the electron-donating orbital in the water dimer. Unlike rigid sp^3 lone pairs, the COVP donor changes its orientation according to the relative positions of the two molecules. A single p-like lone pair is usually the dominant donor, although at the geometry of a bifurcated hydrogen bond, the CT contribution becomes small and two donor orbitals contribute.

Keywords: charge transfer · density functional calculations · hydrogen bonds · molecular orbitals · water chemistry

[1] a) G. Desiraju, T. Steiner, *The Weak Hydrogen Bond in Structural Chemistry and Biology*, Oxford University Press, New York, **1999**; b) G. A. Jeffrey, *An Introduction to Hydrogen Bonding*, Oxford University Press, Oxford, **1997**; c) S. Scheiner, *Hydrogen Bonding: A Theoretical Perspective*, Oxford University Press, Oxford, **1997**.

[2] a) E. D. Isaacs, A. Shukla, P. M. Platzman, D. R. Hamann, B. Barbiellini, C. A. Tulk, *Phys. Rev. Lett.* **1999**, *82*, 600–603; b) T. K. Ghanty, V. N. Staroverov, P. R. Koren, E. R. Davidson, *J. Am. Chem. Soc.* **2000**, *122*, 1210–1214.

[3] F. Weinhold in *Encyclopedia of Computational Chemistry, Vol. 3* (Eds.: P. V. Schleyer, N. L. Allinger, T. Clark, J. Gasteiger, P. A. Kollman, H. F. Schaefer III, P. R. Schreiner), Wiley, New York, **1998**, pp. 1792–1811.

[4] E. D. Glendening, A. Streitwieser, *J. Chem. Phys.* **1994**, *100*, 2900–2909.

[5] F. Weinhold in *Advances in Protein Chemistry, Peptide Solvation and H-Bonds, Vol. 72*, Elsevier, Amsterdam. **2006**, pp. 121–155.

[6] a) G. K. Schenter, E. D. Glendening, *J. Phys. Chem.* **1996**, *100*, 17152–17156; b) E. D. Glendening, *J. Phys. Chem. A* **2005**, *109*, 11936–11940.

[7] a) K. Kitaura, K. Morokuma, *Int. J. Quantum Chem.* **1976**, *10*, 325–340; b) P. S. Bagus, K. Hermann, C. W. Bauschlicher, *J. Chem. Phys.*

1984, *80*, 4378–4386; c) P. S. Bagus, F. Illas, *J. Chem. Phys.* **1992**, *96*, 8962–8970.
[8] a) W. J. Stevens, W. H. Fink, *Chem. Phys. Lett.* **1987**, *139*, 15–22; b) W. Chen, M. S. Gordon, *J. Phys. Chem.* **1996**, *100*, 14316–14328.
[9] J. P. Piquemal, A. Marquez, O. Parisel, C. Giessner-Prettre, *J. Comput. Chem.* **2005**, *26*, 1052–1062.
[10] a) B. Guillot, *J. Mol. Liq.* **2002**, *101*, 219–260; b) G. Robinson, S.-B. Zhu, S. Singh, M. W. Evans, *Water in Biology, Chemistry and Physics. Experimental Overviews and Computational Methodologies*, World Scientific, Singapore, **1996**.
[11] P. Wernet, D. Nordlund, U. Bergmann, M. Cavalleri, M. Odelius, H. Ogasawara, L. A. Naslund, T. K. Hirsch, L. Ojamae, P. Glatzel, L. G. M. Pettersson, A. Nilsson, *Science* **2004**, *304*, 995–999.
[12] A. K. Soper, *J. Phys. Condens. Matter* **2005**, *17*, S3273-S3282.
[13] a) J. D. Smith, C. D. Cappa, K. R. Wilson, B. M. Messer, R. C. Cohen, R. J. Saykally, *Science* **2004**, *306*, 851–853; b) J. D. Smith, C. D. Cappa, B. M. Messer, W. S. Drisdell, R. C. Cohen, R. J. Saykally, *J. Phys. Chem. B* **2006**, *110*, 20038–20045; c) Y. A. Mantz, B. Chen, G. J. Martyna, *J. Phys. Chem. B* **2006**, *110*, 3540–3554; d) D. Prendergast, G. Galli, *Phys. Rev. Lett.* **2006**, *96*; e) T. Head-Gordon, M. E. Johnson, *Proc. Natl. Acad. Sci. USA* **2006**, *103*, 7973–7977; f) T. Head-Gordon, S. W. Rick, *Phys. Chem. Chem. Phys.* **2007**, *9*, 83–91.
[14] R. Z. Khaliullin, E. A. Cobar, R. C. Lochan, A. T. Bell, M. Head-Gordon, *J. Phys. Chem. A* **2007**, *111*, 8753–8765.
[15] R. Z. Khaliullin, A. T. Bell, M. Head-Gordon, *J. Chem. Phys.* **2008**, *128*, 184112.
[16] a) H. Stoll, G. Wagenblast, H. Preuss, *Theor. Chim. Acta* **1980**, *57*, 169–178; b) E. Gianinetti, M. Raimondi, E. Tornaghi, *Int. J. Quantum Chem.* **1996**, *60*, 157–166; c) T. Nagata, O. Takahashi, K. Saito, S. Iwata, *J. Chem. Phys.* **2001**, *115*, 3553–3560.
[17] R. Z. Khaliullin, M. Head-Gordon, A. T. Bell, *J. Chem. Phys.* **2006**, *124*, 204105.
[18] Y. R. Mo, J. L. Gao, S. D. Peyerimhoff, *J. Chem. Phys.* **2000**, *112*, 5530–5538.
[19] Y. Shao, L. F. Molnar, Y. Jung, J. Kussmann, C. Ochsenfeld, S. T. Brown, A. T. B. Gilbert, L. V. Slipchenko, S. V. Levchenko, D. P. O'Neill, R. A. DiStasio, R. C. Lochan, T. Wang, G. J. O. Beran, N. A. Besley, J. M. Herbert, C. Y. Lin, T. Van Voorhis, S. H. Chien, A. Sodt, R. P. Steele, V. A. Rassolov, P. E. Maslen, P. P. Korambath, R. D. Adamson, B. Austin, J. Baker, E. F. C. Byrd, H. Dachsel, R. J. Doerksen, A. Dreuw, B. D. Dunietz, A. D. Dutoi, T. R. Furlani, S. R. Gwaltney, A. Heyden, S. Hirata, C. P. Hsu, G. Kedziora, R. Z. Khalliulin, P. Klunzinger, A. M. Lee, M. S. Lee, W. Liang, I. Lotan, N. Nair, B. Peters, E. I. Proynov, P. A. Pieniazek, Y. M. Rhee, J. Ritchie, E. Rosta, C. D. Sherrill, A. C. Simmonett, J. E. Subotnik, H. L. Woodcock, W. Zhang, A. T. Bell, A. K. Chakraborty, D. M. Chipman, F. J. Keil, A. Warshel, W. J. Hehre, H. F. Schaefer, J. Kong, A. I. Krylov, P. M. W. Gill, M. Head-Gordon, *Phys. Chem. Chem. Phys.* **2006**, *8*, 3172–3191.
[20] a) R. S. Mulliken, *J. Chem. Phys.* **1955**, *23*, 1841–1846; b) P. O. Lowdin, *J. Chem. Phys.* **1950**, *18*, 365–375; c) A. E. Reed, R. B. Weinstock, F. Weinhold, *J. Chem. Phys.* **1985**, *83*, 735–746.
[21] Although DFT is generally not suited for the calculation of virtual orbital eigenvalues the HOMO–LUMO gap in water is relatively well reproduced with modern density functionals. See, for example, G. Zhang, C. B. Musgrave, *J. Phys. Chem. A* **2007**, *111*, 1554–1561.
[22] M. Sharma, Y. D. Wu, R. Car, *Int. J. Quantum Chem.* **2003**, *95*, 821–829.

Received: October 13, 2008
Published online: December 10, 2008

